Processing time: 01.04.2022 – 31.03.2022

Review and Declaration

This thesis has been accepted by the first reviewer of the master thesis.

Karlsruhe, TBD

Prof. Dr. Ralph Engel

I declare that the work in this thesis was carried out in accordance with the requirements of the university's regulations and that it has not been submitted for any other academic award. Except where indicated by specific reference in the text, the work is the candidate's own work. Work done in collaboration with, or with the assistance of, others is indicated as such.

Karlsruhe, TBD

Paul Filip

Contents

1 The Pierre Auger Observatory

Located on the argentinian high-plains of Pampa Amarilla, the Pierre Auger observatory is a hybrid detector designed to detect and study cosmic rays of the highest energies. With an effective area of $3000\,\mathrm{km}^2$ it is by far the largest experiment of its kind [**DesignReport**].

Altough first proposed in 1992, it took 18 years until the idea of a large scale experiment to detect cosmic rays matured and construction of the first prototype started near Mendoza [**AugerTimeline**]. Some further 20 years later, the Pierre Auger collaboration has co-authored over publications and continues to advance research in astroparticle physics. It does this via a hybrid approach, combining measurements of a **S**urface **D**etector (SD) as well as a **F**louresence **D**etector (FD). Additional machinery, such as the e**X**treme (XLF) and **C**entral **L**aser **F**acility (CLF), is installed to monitor atmospheric variables. This improves the overall systematic accuracy of predictions made by the experiment. An overview of the site can be seen in **??**. Data measured by the FD, SD and the atmospheric monitors is sent to a **C**entral **D**ata **A**cquisition **S**ystem (CDAS) located in the nearby town of Malargüe.

This chapter offers a brief look into the measurement principle and setup of the observatory. Information regarding the fluoresence detector can be found in **??**. The SD is described in **??**. A more in depth read on detector specifications and design choices is represented by the Pierre Auger observatory design report [**DesignReport**], where a lot of information stated in this chapter is conglomerated from. Notes on the event reconstruction are listed in **??** and summarized from [**SDReconstruction**] and [**FDReconstruction**].

1.1 Fluoresence Detector (FD)

The FD consists of a total of 27 fluoresence telescopes (eyes) at 4 different sites. Each eye monitors a 30° x 30° window of the sky at a resolution of $\approx 0.5\,\frac{\mathrm{px}}{\mathrm{deg}^2}$. This results in an effective FOV of roughly 180° x 30° per FD station, with an exception of Coihueco, where three additional telescopes - HEAT (**H**igh **E**levation **A**uger **T**elescope) - are installed to enable monitoring of higher zenith angles ($30° \leq \theta \leq 60°$) and increase sensitivity for showers of lower energies (compare **??**).

The individual telescopes consist of 3.6 m by 3.6 m, convex mirrors. They reflect incoming light onto a set of 440 photomultipliers (PMTs), each corresponding to one pixel in the resulting image seen by an eye. Since the setup needs to be extremely sensitive to UV light in order to detect flouresence caused by extensive air showers,

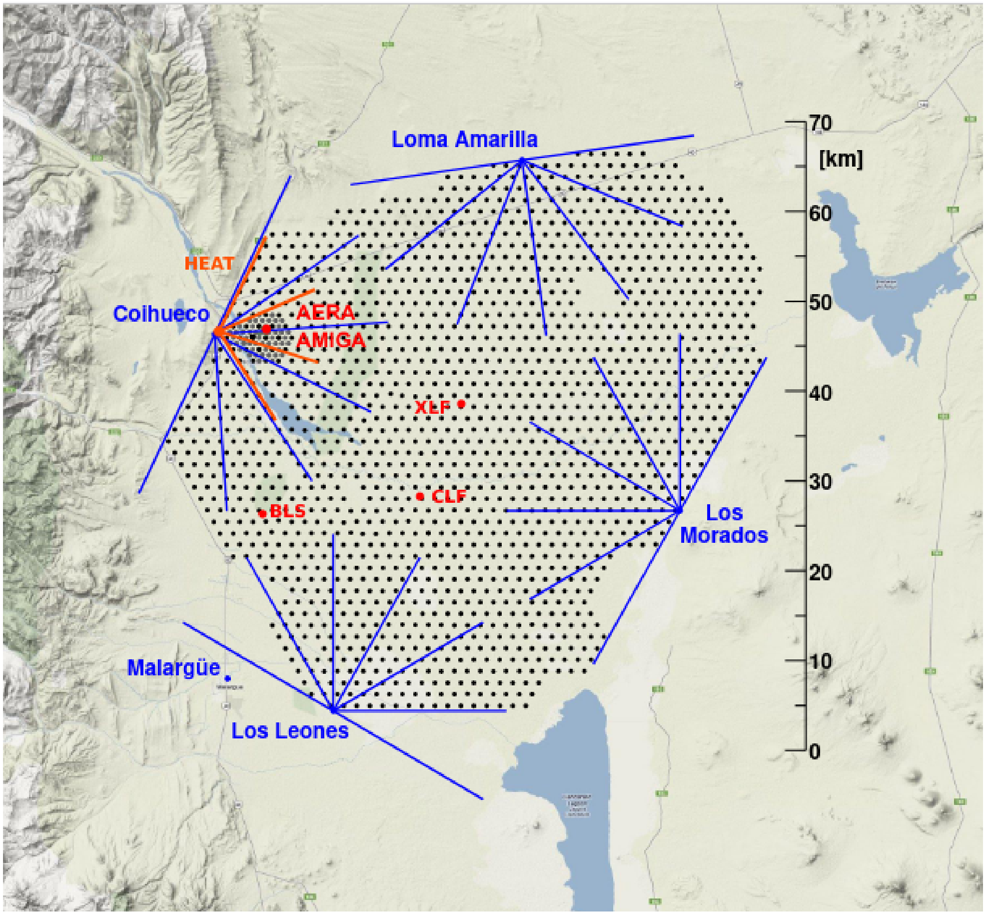

Figure 1.1: Overview of the Pierre Auger observatory. The four different FD sites (respective FOV shown with blue lines) sit at the edge of the detector area and monitor the night sky above the SD array consisting of 1600 water tanks (black dots). A denser spacing of stations near Coihueco is equipped with additional electronics such as e.g. radio antennas (AERA) and muon detectors (AMIGA). Image taken from [**AugerArray**]

.

its operation is limited to the relatively noise free moonless astronomical nights (Sun $\measuredangle$ Horizon $\lesssim -18°$). When the FD is operational, this allows the observation of the longitudinal propagation of a shower instead of just its' footprint (as seen by the SD).

1.2 Surface Detector (SD)

PICTURE!

The SD consists of 1600 individually operating stations, spaced apart on a hexagonal grid with a standard 1.5 km spacing. Each station is made up of a main tank filled with 12 000 L of purified water and reflective inner walls, a solar panel and batteries for power management, as well as an antenna for communication. Within each tank three PMTs detect Cherenkov light originating from shower particles, these are together with the tank referred to as **W**ater **C**herenkov **D**etectors (WCDs). With the (at the time of this work) ongoing AugerPrime upgrade, each station is additionally equipped with a **s**mall **PMT** (sPMT), **S**urface **S**cintillator **D**etector (SSD), and radio antenna atop the tank. This allows for the recording of stronger signals, finer separation of electromagnetic and muonic shower component and detection of highly inclined air showers respectively [**AugerPrime**, **horandel2020precision**].

1.2.1 Data acquisition (DAQ)

Onboard electronics, the **U**pgraded **U**nified **B**oard (UUB), or more precisely six 10-bit **F**lash **A**nalog-to-**D**igital-**C**onverters (FADCs) read out measurement data from the PMTs at a sampling rate of 120 MHz ($\approx$ 8.33 ns binning) [**verzi2013energy**]. This is done in a two-fold way. Three FADCs digitize the PMTs dynode voltage, resulting in the **H**igh**G**ain (HG) output. Three FADCs monitor the anode voltage to form the **L**ow **G**ain (LG) output, which can be analyzed if the HG output exceeds a value of 2^{10} ADC counts and becomes saturated. This effectively enables the measurement of both large ($\geq \mathcal{O}(10^3)$ particles hitting the tank) as well as small shower signals ($\mathcal{O}(1)$ particle hitting the tank) with sufficient accuracy. Once an FADC bin has been recorded and checked for possible triggers (c.f. **??**) it is written to a ring buffer. If a trigger is issued, the corresponding chunk in the ring buffer ($\approx$ 4.992 µs (599 bins) before and 12.07 µs (1448 bins) after a trigger, 2047 + 1 bins total), the measured trace, can be analyzed in order to calibrate a station in the array (**??**) or processed by a higher-level CPU for event reconstruction purposes (see **??**).

1.2.2 Calibration

While each station is equipped with the same electronics and runs the same analysis software, variables like the position in the field, station age or slight changes in the manufacturing/installation process cause different stations to age differently. Over the lifetime of the array such differences can sum into potentially drastic discrepancies in gathered data. Put simply, an extensive air shower will look different both to different WCDs at the same time as well as the same WCD at different times. To account for this, measurements are standardized across all stations. ADC counts are related to a **V**ertical **E**quivalent of through-going **M**uons (VEM) that would result in the same signal strength. In this fashion, the maximum response that is generated by a PMT from one vertically through-going muon is defined as 1 $\mathrm{VEM}_{\mathrm{Peak}}$. The total deposited charge (equivalent to the integral of the response) is defined as 1 $\mathrm{VEM}_{\mathrm{Ch.}}$. The conversion factor between ADC counts and $\mathrm{VEM}_{\mathrm{Peak}}$ and $\mathrm{VEM}_{\mathrm{Ch.}}$ is estimated from data and continuously updated separately for each station. Note that due to the limited computational resources of the WCD, a simplified, rate-based approach is chosen for calibration in the field (Online algorithm), this stands in contrast to the more physics-driven methods used during event reconstruction (Oflline algorithm). In any case, both algorithms are listed here and discussed in more detail in [**tobiasBaseline**], [**bertou2006calibration**], .

Online algorithm

Baseline

Once the baseline

Offline algorithm

For event reconstruction, a first baseline estimate of a WCD PMT is predicted from the beginning and end of a 2048 bin (17.06 µs) long trace. The mode m as well as standard deviation σ of the first (last) 300 bins is calculated. All bins larger or smaller than $m \pm 2\sigma$ are truncated and removed from the trace window. The value of m, σ is consequently updated and the procedure repeated until a convergence is reached and no further cut is necessary. The best estimate B_{front} (B_{end}) for the front (end) of the trace at this point is given by the mean value of all remaining bins. It's statistic uncertainty $\sigma_{B_{\mathrm{front}}}$ ($\sigma_{B_{\mathrm{end}}}$) is given by the standard deviation of the remaining bins. The baseline between the flat front and end estimate is then interpolated based on the difference $\Delta B = B_{\mathrm{end}} - B_{\mathrm{front}}$.

- **Rejection of anomalous upward fluctuations $\frac{\Delta \mathbf{B}}{\sigma_{\Delta \mathbf{B}}} \geq +5$:**

  B_{end} being higher than Bfront often indicates errors in the electronic readout or defect components in the measurement chain. There exists no physical reason why the end baseline should be (significantly) higher than the front. Consequently, traces where this is the case are ignored during event reconstruction.

- **Constant approximation for small upward fluctuations $+5 > \frac{\Delta \mathbf{B}}{\sigma_{\Delta \mathbf{B}}} \geq 0$:**

  Small fluctuations of the baseline are expected and the norm. If these fluctuations are positive ($B_{\mathrm{end}} > B_{\mathrm{front}}$) the method of calculating the mode, truncating outliers and repeating both steps is applied to the entire length of the signal, resulting in a constant baseline estimate B across the trace.

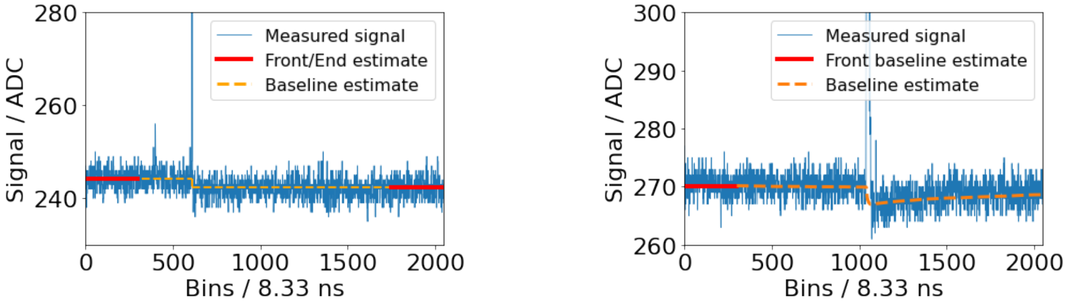

(a) Step-function approximation **(b) Charge-linear interpolation**

Note that the signal undershoot is greatly exaggerated for visualization purposes in both examples. **a)** A simple step function is sufficient to accurately model a PMTs' noise level at small downward fluctuations. **b)** For larger discrepancies, the more involved charge-linear interpolation is used.

- **Step-function approximation for small downward fluctuations $0 > \frac{\Delta B}{\sigma_{\Delta B}} \geq -1$:**

  Unlike positive fluctuations, negative fluctuations ($B_{\text{end}} < B_{\text{front}}$) can have a physical significance. Due to the undershoof of PMTs after detecting a signal in the WCD (compare [**glietta2008recovery**]), the baseline estimate decreasing towards the end of the trace often indicates the presence of shower particles within the tank. For this reason, downward fluctuations are handled differently from upward ones. If the fluctuations are sufficiently small, the baseline across the trace is estimated as a simple step-function; The trace is separated into two parts along its' maximum ADC value. The front part (i.e. before the max. value) has the baseline B_{front}, while the rear part is estimated by B_{end}. An example of this is shown in **??**.

- **Charge-linear approximation for large undershoots $-1 \geq \frac{\Delta B}{\sigma_{\Delta B}}$:**

  For larger undershoots, the baseline is interpolated bin by bin based on the deposited charge in the detector. Starting from the front baseline estimate B_{front} for the bins 0-300, the remaining baseline (bins 301-2048) This is visualized in **??**.

1.2.3 Trigger procedure

1.3 Event Reconstruction